

# MUC1-induced immunosuppression in colon cancer can be reversed by blocking the PD1/PDL1 signaling pathway

YINGHUI ZHANG<sup>1\*</sup>, XIANGQIAN DONG<sup>2\*</sup>, LIPING BAI<sup>1</sup>, XUEQIN SHANG<sup>3</sup> and YUJIAN ZENG<sup>4</sup>

<sup>1</sup>Department of Gastroenterology, The Fourth Affiliated Hospital of Kunming Medical University, Kunming, Yunnan 650021; <sup>2</sup>Department of Gastroenterology, The First Affiliated Hospital of Kunming Medical University, Yunnan Institute of Digestive Diseases, Kunming, Yunnan 650032; <sup>3</sup>Department of Medical Oncology, The Fourth Affiliated Hospital of Kunming Medical University, Kunming, Yunnan 650021; <sup>4</sup>Department of Gastrointestinal Surgery, The First Affiliated Hospital of Kunming Medical University, Kunming, Yunnan 650032, P.R. China

Received March 10, 2020; Accepted August 20, 2020

DOI: 10.3892/ol.2020.12180

**Abstract.** Mucin1 (MUC1) upregulation in colon cancer has been linked to poor patient outcomes and advanced stage at diagnosis. This is partially due to MUC1-mediated inhibition of T-cell proliferation affecting efficient lysis by cytotoxic lymphocytes, which contributes to escape from immune surveillance. In the present study, human colorectal cancer tissues were collected, and MUC1-positive and MUC1-negative colon cancer mouse models were prepared; subsequently, the number and function of immune cells in tumor tissues were measured using flow cytometry. The present study revealed that MUC1, as a tumor-associated antigen, can recruit more tumor-infiltrating lymphocytes into the tumor microenvironment compared with MUC1-negative colon cancer, but that these cells could not serve antitumor roles. Conversely, the present study demonstrated that MUC1-positive colon cancer attracted more regulatory T cells (Treg cells), myeloid-derived suppressor cells (MDSCs) and tumor-associated macrophages (TAMs) to the tumor site than MUC1-negative colon cancer. Furthermore, the data suggested that programmed death protein 1 (PD1)-programmed death ligand 1 (PDL1) expression is greater in MUC1-positive colon cancer. Blocking the

PD1-PDL1 signaling pathway reduced the percentage of Treg cells, MDSCs and TAMs in the tumor microenvironment, enhanced T-cell cytotoxicity and inhibited tumor growth, prolonging the survival time of MUC1-positive tumor-bearing mice. Therefore, the present study elucidated the role of MUC1 in tumor immune escape and provides a foundation for the application of PDL1 inhibitors to MUC1-positive colon cancer.

## Introduction

Colon cancer is one of the most common types of cancer and the second leading cause of cancer-related mortality worldwide (1). The tumor-associated antigen, mucin1 (MUC1), is highly expressed in colon cancer and has been linked to poor outcomes (2,3). MUC1 is a transmembrane molecule that is expressed by the glandular epithelial cells of the prostate, stomach, duodenum, pancreas and colon, and is also found in hematopoietic cells (4). It has a heavily glycosylated extracellular domain (4,5). The abnormal glycosylation and upregulation of MUC1 in human epithelial carcinoma has aroused great interest as a candidate tumor marker and potential tumor-killing target (5). Compared with fully glycosylated MUC1, hypoglycosylated forms and upregulated MUC1 have pivotal roles in the transcriptional regulation of genes associated with immune responses, tumor invasion, apoptosis, angiogenesis, proliferation and inflammation (6). High expression levels of MUC1 are associated with a poor prognosis in patients with colorectal cancer (7). In a breast cancer animal model, intravenous injection of MUC1 induces immunosuppression and accelerates tumor-bearing mouse death (8). Serum MUC1 expression levels are also associated with immunosuppression in patients with metastatic adenocarcinoma treated with active specific immunotherapy (8-10). In addition, MUC1 causes apoptosis of activated human T-cells, which inhibits the proliferation of human T cells and cytotoxic lymphocyte-target cell interactions (11,12). However, the pro-tumor and immunosuppressive roles of MUC1 in colon cancer have not been fully elucidated.

The programmed death protein 1 (PD1)-programmed death ligand 1 (PDL1) signaling pathway is involved in tumor immune escape, in which the tumor cells evade host immune

---

*Correspondence to:* Dr Yujian Zeng, Department of Gastrointestinal Surgery, The First Affiliated Hospital of Kunming Medical University, 295 Xichang Road, Kunming, Yunnan 650032, P.R. China  
E-mail: zengyujian666@163.com

\*Contributed equally

*Abbreviations:* MUC1, mucin1; Treg cells, regulatory T cells; MDSCs, myeloid-derived suppressor cells; TAM, tumor-associated macrophage; PDL1, programmed death ligand 1; PD1, programmed cell death 1; TILs, tumor-infiltrating lymphocytes; CTL, cytotoxic T cell

*Key words:* MUC1, colon cancer, immunotherapy, PDL1, tumor microenvironment

surveillance by inhibiting the toxicity of T cells via the PD1-PDL1 signaling pathway (13). Immunogenic tumor cells might induce anergy of tumor-specific T cells by expressing PDL1 on their surfaces (14). A variety of factors induce PDL1 expression in tumor cells and antigen-presenting cells, which includes the inflammatory cytokines IFN- $\gamma$  and IL-17A (15). MUC1, as a tumor-associated antigen, recruits white blood cells into the tumor microenvironment, which results in the secretion of inflammatory cytokines (16). However, it is unclear whether the tumor cells upregulate PDL1 expression via MUC1 to escape immune surveillance. In the present study, the mechanisms underlying PDL1 expression in MUC1-positive tumor tissue were explored, and the potential of targeting PDL1 to inhibit the progression of MUC1-overexpressing colon cancer in mice was demonstrated. A clearer understanding of this process may help to define the role of MUC1 in promoting tumor immune escape and provide key information to support immunotherapy through targeting the PDL1-PD1 signaling pathway in MUC1-positive colon cancer.

## Materials and methods

**Mice and cell lines.** Female BALB/c mice (100 mice; 8 weeks old; 18–21 g) and female nu/nu mice (40 mice; 8 weeks old; 18–22 g) were purchased from the Animal Experiment Center of Kunming Medical University. All animals used in the present study were kept under specific pathogen-free conditions, in a temperature-controlled environment (20–23°C) with 40–60% humidity and with a 12-h light/dark cycle, with food and water freely available. Colon cancer SW480 (human) and CT26 (mouse) cells, sourced from the American Type Culture Collection, were cultured in DMEM supplemented with 10% FBS and with 2 mM L-glutamine (all Gibco; Thermo Fisher Scientific, Inc.) at 37°C with 5% CO<sub>2</sub>.

**Patients and sample collection.** To study the association between the survival time of patients with colorectal cancer and MUC1 expression in tumor tissues, a discovery cohort of 230 patients with colorectal cancer (dataset: Colon and Rectal Cancer) was obtained from The Cancer Genome Atlas (TCGA) database available from University of California Santa Cruz Xena (<https://xenabrowser.net/>) (17,18). To study the role of immune cells in colorectal cancer tissues, colon cancer specimens were collected from 33 male patients (Table I) who underwent open surgery at The First Affiliated Hospital of Kunming Medical University (Kunming, China) between April 2017 and August 2018. The mean age of the patients was 56 years old. Individuals with primary colon cancer who had not received any treatment were deemed eligible for the present study. The clinical diagnosis was confirmed by histopathological detection. MUC1 expression was detected using immunohistochemistry (IHC). The present study was approved by the Ethics Committee of The First Affiliated Hospital of Kunming Medical University (approval no. KMU20160901) and conformed with the ethical standards of the World Medical Association Declaration of Helsinki. All patients provided written informed consent.

**Establishment of a stable cell line expressing MUC1.** The plasmid pRP[Exp]-EGFP/Puro-CAG>hMUC1[NM\_001371720.1]

was purchased from VectorBuilder, Inc. The human *MUC1* gene was amplified and subcloned in-frame between the *NheI* and *HindIII* restriction sites of *pcDNA3.1(-)/Myc-His A* (cat. no. V855-20; Invitrogen; Thermo Fisher Scientific, Inc.). A total of 5x10<sup>5</sup> CT26 or SW480 cells/well in 500  $\mu$ l DMEM without antibiotics were plated in 6-well plates, and then cells were transfected for 24 h with *pcDNA3.1(-)/Myc-His-muc1* (2  $\mu$ g) or *pcDNA3.1(-)/Myc-His* (2  $\mu$ g) using Lipofectamine™ 2000 transfection reagent (Thermo Fisher Scientific, Inc.) according to the manufacturer's protocols. The transfected cells were cultured in DMEM with 10% FBS containing G418 (1 mg/ml; cat. no. 10131027; Thermo Fisher Scientific, Inc.) to establish stable cell lines expressing hMUC1. MUC1<sup>+</sup>CT26 and MUC1<sup>+</sup>SW480 tumor cells were sorted using flow cytometry and maintained in medium containing the antibiotic G418 (10% FBS; 1 mg/ml G418). The CT26 and SW480 cells, which were transfected with *pcDNA3.1(-)/Myc-His* as aforementioned, were also maintained in the same medium containing G418 (10% FBS; 1 mg/ml G418). Human MUC1 expression was confirmed by flow cytometry and western blotting one month after cells were transfected.

**Western blotting.** The cells were lysed in RIPA buffer (Beyotime Institute of Biotechnology) for 10 min on ice, and then the supernatant was collected by centrifugation (250 x g; 4°C; 5 min) to remove cell debris. The protein concentration was measured using a Bradford assay (Bio-Rad Laboratories, Inc.). Protein samples (20  $\mu$ g/well) were loaded on a 10% (w/v) tris-HCl SDS-PAGE gel for electrophoresis and transferred to PVDF membranes (cat. no. 3010040001; Sigma-Aldrich; Merck KGaA), which were blocked in 5% bovine serum albumin (Sigma-Aldrich; Merck KGaA) for 45 min at room temperature. Subsequently, the membrane was probed with anti-MUC1 (1:3,000; cat. no. ab36690; Abcam), anti-PDL1 (1:1,000; cat. no. ab238697; Abcam) or anti- $\beta$ -actin (1:1,000; cat. no. ab8226; Abcam) primary antibodies at 4°C overnight. The signal was detected using a goat anti-mouse secondary antibody (1:3,000; cat. no. ab205719; Abcam) conjugated to horseradish peroxidase at room temperature for 1 h. Band signals were visualized using the Immobilon Western Chemiluminescent substrate (Merck KGaA) and detected using the Odyssey CLx (LI-COR Biosciences). Furthermore, PDL1 expression in tumor tissues was analyzed using Gel-Pro Analyzer 3.0 (Media Cybernetics, Inc.).

**IHC.** The expression levels of MUC1 in colon cancer tissues were determined using IHC. Briefly, 10% formalin-fixed (8 h at room temperature), paraffin-embedded sections (4- $\mu$ m-thick) were cut using a microtome, mounted on silanized glass slides and dried overnight at 37°C. A graded alcohol series (100 and 70%) and distilled water were used to deparaffinize and rehydrate the slides. Slides containing tumor sections were incubated for 30 min in citrate buffer (pH 6.0) at 96°C, followed by a 1-h incubation at room temperature with blocking buffer (10% FBS in PBS). Slides were then incubated in a humidified chamber at room temperature for 1 h with rabbit anti-human MUC1 monoclonal antibody (1:1,000; cat. no. ab109185; Abcam), followed by incubation in a humidified chamber at room temperature for 30 min

Table I. Demographic data of recruited patients with colorectal cancer.

Characteristic	MUC1 <sup>high</sup>	MUC1 <sup>low</sup>
Age range, years	45-72	47-76
Metastasis	10 (30.3) <sup>a</sup>	9 (27.3) <sup>a</sup>
Stage		
I	8	6
II	10	9

<sup>a</sup>Numbers inside parentheses are percentages of patients. Tumours with >90 MUC1-producing cells (i.e., the mean of the cohort) were considered as 'high'; those with ≤90 infiltrating MUC1-producing cells were considered as 'low'. MUC1, mucin1.

with a horseradish peroxidase-labeled anti-rabbit secondary antibody (1:3,000; cat. no. ab7090; Abcam). The sections were developed using 3,3'-diaminobenzidine tetrahydrochloride. Antibody staining in the tissue sections was observed using light microscopy (Olympus Corporation). For quantification, cells stained with MUC1 were manually counted at a magnification of x400 in five high-power fields of each tumor tissue. The average number of cells stained with MUC1 in each tumor sample was counted to reflect the number of MUC1-expressing cells in the tumor. Similarly to PDL1 expression in tumor tissues of a previous study (15), tumors with >90 and ≤90 MUC1-expressing cells were considered to have high and low expression, respectively.

**Cytokine-specific ELISA.** ELISA assays were used to analyze IL-10, IL-17A, TNF- $\alpha$ , TGF- $\beta$  and IFN- $\gamma$  levels in the tumor microenvironment of mice and patients with colon cancer. Fresh tumor tissues were isolated from patients with colon cancer and tumor-bearing mice. The tumor tissues were homogenized in PBS (0.1 g tissue/ml). The supernatants were collected by centrifugation (1,200 x g; 4°C; 10 min) for analysis of cytokine expression levels using mouse IL-10 (cat. no. 88-7105-22), IL-17A (cat. no. 88-7371-22), TNF- $\alpha$  (cat. no. 88-7324-22), TGF- $\beta$  (cat. no. 88-8350-22) and IFN- $\gamma$  (cat. no. 88-7314-22), or human IL-10 (cat. no. KAC1321), IL-17A (cat. no. BMS2017), TNF- $\alpha$  (cat. no. 88-7346-22), TGF- $\beta$  (cat. no. 88-8350-22) and IFN- $\gamma$  (cat. no. 88-7316-22) ELISA kits (Thermo Fisher Scientific, Inc.) according to the manufacturer's protocols.

**Cell proliferation assay.** To assess the number of living cells, 1-2x10<sup>4</sup> CT26/MUC1 or SW480/MUC1 cells were plated and cultured with 10% FBS-supplemented DMEM containing G418 (1 mg/ml) for 7 days. CT26/vector or SW480/vector cells were cultured as negative controls. Proliferation was measured using trypan blue exclusion. In brief, the cells were centrifuged at 4°C for 5 min at 100 x g and then resuspended in 1 ml PBS. One part 0.4% trypan blue was mixed with one part cell suspension and incubated for ~3 min at room temperature. A drop of the trypan blue/cell mixture was applied to a hemocytometer and the unstained (viable) and stained (nonviable) cells were counted separately with a binocular microscope using the

hemocytometer. The number of living cells was counted, and the proliferation of cells was analyzed.

**Tumor implantation.** CT26/MUC1 or CT26/vector cells (1x10<sup>6</sup> cells/200  $\mu$ l PBS/body) were transplanted subcutaneously into the right flank of BALB/c mice; SW480-MUC1 or SW480/vector cells (2x10<sup>6</sup> cells/200  $\mu$ l PBS/body) were transplanted subcutaneously into the right flank of nu/nu mice to establish a mouse model of MUC1-positive and MUC1-negative colon cancer. The tumor diameters were measured from day 7 after tumor implantation. The treatment of mice was approved by the Institutional Animal Care and Use Committee of Kunming Medical University (approval no. KMU20170121).

For the analysis of survival time of tumor-bearing mice (the experiments were conducted between January 2017 and November 2019), tumor size (using microcalipers) and bodyweight were measured every 2-3 days. The volumes were calculated as: (length x width x depth)/2. Mice in cages were euthanized by CO<sub>2</sub> exposure for 5 min (flow rate, 3 l/min; 23% chamber vol/min) when tumor diameters reached 12 mm, according to the Animal Care and Use Committee Guidelines (19), to minimize the suffering of the tumor-bearing mice. The mice were considered dead when the respiration, heartbeat and reflex activity had ceased. The survival rate of tumor-bearing mice was then evaluated. For surface molecules and intracellular cytokine analysis (the experiments were conducted between March 2017 and June 2017), the CT26 tumor-bearing mice were sacrificed on day 26 after tumor cell inoculation and surface and intracellular cytokine staining patterns of myeloid-derived suppressor cells (MDSCs) and T cells were analyzed using flow cytometry.

For the treatment (the experiments were conducted between April 2018 and August 2018), the tumor-bearing mice were anesthetized with 2% pentobarbital (45 mg/kg) via intraperitoneal injection, and then injected intravenously with an anti-mouse PDL1 antibody (200  $\mu$ g/mouse; BE0101; Bio X Cell) four times at 3-day intervals, after palpable tumors (3-5 mm in diameter) had formed. The tumor volumes and survival rates of tumor-bearing mice were evaluated. In another experimental set (the experiments were conducted between April 2018 and June 2018), the tumor-bearing mice were euthanized on the third day after the end of PD1 antibody treatment. Surface and intracellular staining of cells was performed, and cytokine-producing T cells, MDSCs and tumor-associated macrophages (TAMs) were analyzed using flow cytometry.

In some experiments (conducted between April 2018 and November 2018) a rat anti-mouse CD8 antibody (500  $\mu$ g/mouse; cat. no. BE0223; Bio X Cell) or isotype control rat IgG1 (250  $\mu$ g/mouse; cat. no. BE0088; Bio X Cell) was injected into the abdominal cavity of the mouse 3 days before the PDL1 antibody treatment, followed by evaluation of tumor volumes and survival rates of tumor-bearing mice.

**Surface and intracellular molecular staining.** Transfected CT26 and CT26/MUC1 cells (2x10<sup>6</sup> cells/well) were stimulated using IL-17A (10 ng/ml; R&D Systems China Co., Ltd.) and IFN- $\gamma$  (10 ng/ml; R&D Systems China Co., Ltd.) at 37°C for 48 h, the cells were then harvested via centrifugation (250 x g; 4°C; 10 min) and counted. Subsequently, the cells

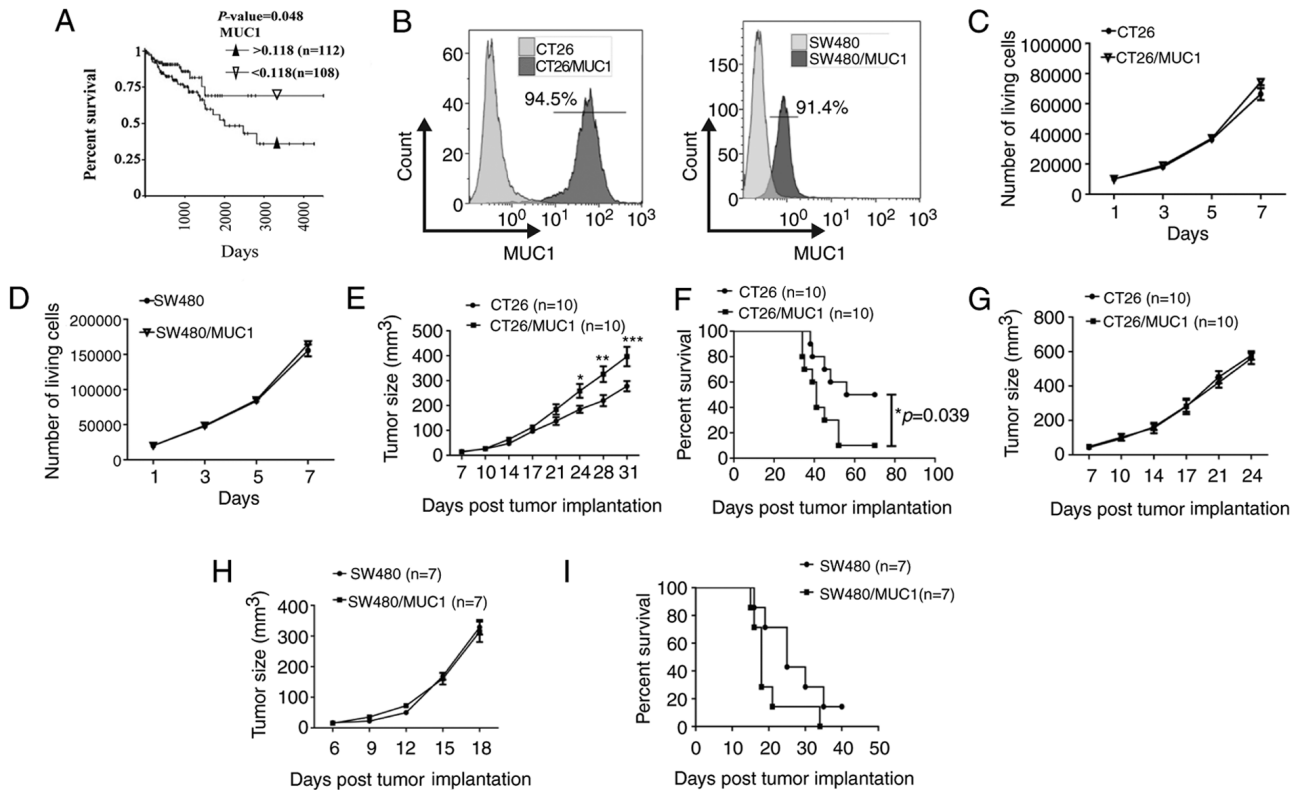


Figure 1. Association between MUC1 expression and overall survival in patients with colon cancer or tumor-bearing mice. (A) Kaplan-Meier curves of overall survival of patients with colon cancer in The Cancer Genome Atlas discovery set divided based on *MUC1* mRNA expression in the total cohort. (B) CT26 (left) and SW480 (right) tumor cells were transfected with *pcDNA3.1(-)/Myc-His-MUC1* and the positive cells were sorted by flow cytometry. The purity of the cells was evaluated by flow cytometry. Briefly, (C)  $1 \times 10^4$  CT26/MUC1 or (D)  $2 \times 10^4$  SW480/MUC1 cells were plated and cultured in G418-containing media for 7 days, and CT26/vector or SW480/vector cells were cultured as negative controls. Cell count was measured using trypan blue exclusion. BALB/c mice were injected subcutaneously with  $1 \times 10^6$  CT26/vector or CT26/MUC1 tumor cells. After 7 days, (E) tumor growth and (F) survival rates ( $n=10$ ) were recorded. Nu/nu mice were injected subcutaneously with (G)  $1 \times 10^6$  CT26/vector or CT26/MUC1 tumor cells ( $n=10$ ), or  $2 \times 10^6$  SW480/vector or SW480/MUC1 tumor cells ( $n=7$ ). After 7 days (H) tumor growth and (I) survival rates were recorded. Data are representative of three replicate experiments. Error bars represent the standard error of the mean. \*\*\* $P < 0.001$ , \*\* $P < 0.01$  and \* $P < 0.05$  vs. model control. MUC1, mucin1.

were stained with PE anti-PDL1 at  $4^\circ\text{C}$  for 30 min (1:100; cat. no. 124308; clone 10F.9G2; BioLegend, Inc.). Fluorescence data were acquired using a CytoFLEX flow cytometer (Beckman Coulter, Inc.) and analyzed using Kaluza software v2.1 (Beckman Coulter, Inc.).

For the surface staining of tumor cells and immune cells, the tumor tissues from tumor-bearing mice or patients with colon cancer were weighed, homogenized and digested with hyaluronidase (2 mg/ml), collagenase type IV (2 mg/ml), and deoxyribonuclease (25  $\mu\text{g}/\text{ml}$ ; Sigma-Aldrich; Merck KGaA) for 50 min at  $37^\circ\text{C}$ . Immune cells were enriched with Ficoll reagent and stained with propidium iodide at  $4^\circ\text{C}$  for 5 min. After counting viable cells, the samples were incubated with an anti-CD16/CD32-blocking Ab (1:100; cat. no. Ab00123-23.0-BT; Absolute Antibody) at  $4^\circ\text{C}$  for 10 min and then stained at  $4^\circ\text{C}$  for 30 min with Brilliant Violet 510<sup>TM</sup> anti-mouse CD45 (1:100; cat. no. 103138; clone 30-F11; BioLegend, Inc.), Brilliant Violet 510<sup>TM</sup> anti-human CD45 (1:100; cat. no. 304036; clone HI30; BioLegend, Inc.), FITC anti-mouse CD4 (1:100; cat. no. 100509; clone RM4-5; BioLegend, Inc.), FITC anti-human CD4 (1:100; cat. no. 317408; clone OKT4; BioLegend, Inc.), FITC anti-mouse CD8a (1:100; cat. no. 100706; clone 53-6.7; BioLegend, Inc.), FITC anti-human CD8a (1:100; cat. no. 301050; clone RPA-T8; BioLegend, Inc.), APC anti-mouse CD279 (PD-1; 1:100; cat. no. 109112; clone

RMP1-30; BioLegend, Inc.), APC anti-human CD279 (PD-1; 1:100; cat. no. 329908; clone EH12.2H7; BioLegend, Inc.), PE anti-mouse/human CD11b (1:100; cat. no. 101207; clone M1/70; BioLegend, Inc.), FITC anti-mouse Ly-6G/Ly-6C (Gr-1; 1:100; cat. no. 108406; clone RB6-8C5; BioLegend, Inc.), FITC anti-human CD66b (1:100; cat. no. 305104; clone G10F5; BioLegend, Inc.), PerCP/Cyanine5.5 anti-mouse F4/80 (1:100; cat. no. 123128; clone BM8; BioLegend, Inc.), PerCP/Cyanine5.5 anti-human CD68 (1:100; cat. no. 333813; clone Y1/82A; BioLegend, Inc.), APC anti-mouse CD274 (B7-H1, PD-L1; 1:100; cat. no. 124311; clone 10F.9G2; BioLegend, Inc.), APC anti-human CD274 (B7-H1, PD-L1; 1:100; cat. no. 329708; clone 29E.2A3; BioLegend, Inc.) or PE anti-human MUC1 (1:1,000; cat. no. ab213337; clone EP1024Y; Abcam). The live cells were gated. Fluorescence data were acquired using a CytoFLEX flow cytometer and analyzed using Kaluza software v2.1.

For the intracellular staining of immune cells,  $1 \times 10^6$  cells/ml were treated with Cell Activation Cocktail containing Brefeldin A (1:1,000; cat. no. 423304; BioLegend, Inc.). After 4 h, the cells were collected and stained with the aforementioned Brilliant Violet 510<sup>TM</sup> - or FITC-conjugated mAbs against mouse or human CD45, CD4 or CD8 mAbs (BioLegend, Inc.) at  $4^\circ\text{C}$  for 30 min. The cells were then fixed with Fixation Buffer (cat. no. 420801; BioLegend, Inc.) in the

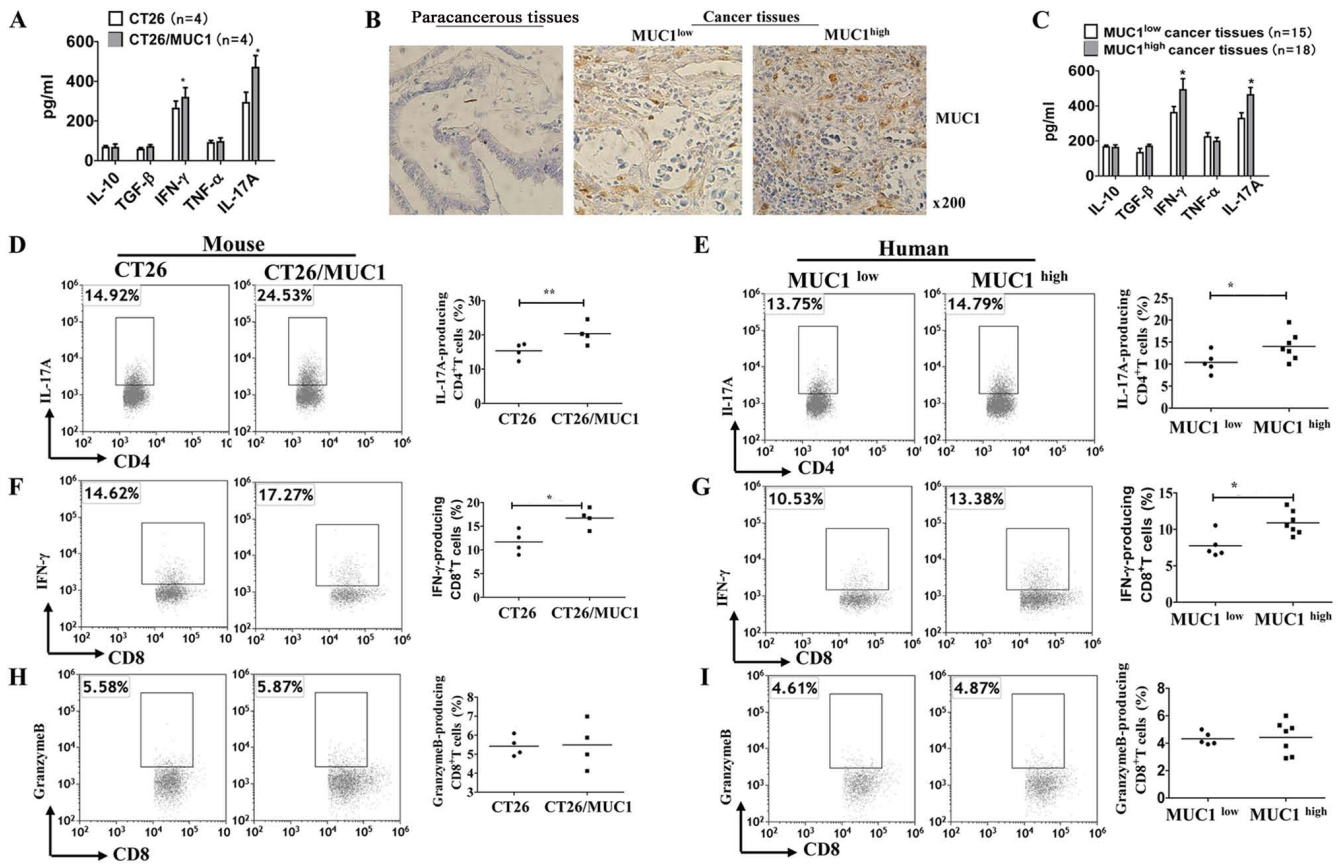


Figure 2. Increased expression levels of inflammatory cytokines in tumor tissues of MUC1-positive tumor-bearing mice and patients with colon cancer expressing MUC1<sup>high</sup>. (A) Tumor tissues were harvested from tumor-bearing mice (n=8). The tumor tissues were homogenized in PBS (0.1 g tissue/ml). The supernatants were collected by centrifugation and the levels of cytokines were analyzed using ELISAs. (B) Representative images of immunohistochemical staining of MUC1-positive tumor tissues from patients with colon cancer. Magnification, x200. (C) Tumor tissues from patients with colon cancer (n=33) were harvested. The tumor tissues were homogenized in PBS (0.1 g tissue/ml). The supernatants were collected by centrifugation and the levels of cytokines were analyzed using ELISAs. The tumors were resected and processed to generate a single-cell suspension. TILs from the tumors were stimulated with a Cell Activation Cocktail with Brefeldin A for 4 h. Percentages of IL-17<sup>+</sup> T-cells among CD4<sup>+</sup>CD45<sup>+</sup> TILs in (D) mice (n=8) and (E) humans (n=12). Percentages of IFN- $\gamma$ <sup>+</sup> T-cells among CD8<sup>+</sup>CD45<sup>+</sup> TILs in (F) mice and (G) humans. Percentages of granzyme B<sup>+</sup> T-cells among CD8<sup>+</sup>CD45<sup>+</sup> TILs in (H) mice and (I) humans. Data are representative of four experiments. Error bars represent the standard error of the mean. \*\*P<0.01 and \*P<0.05 vs. model control. MUC1, mucin1; TILs, tumor-infiltrating lymphocytes.

dark at room temperature for 20 min. Next, the cells were permeabilized with 1X intracellular Staining Permeabilization Wash Buffer (cat. no. 421002; BioLegend, Inc.) and incubated with PE-conjugated anti-IFN- $\gamma$  anti-IL-17 or anti-granzyme B (BioLegend, Inc.) for 30 min at room temperature. For forkhead box P3 (Foxp3) staining, the fixed cells were treated using the True-Nuclear™ Transcription Factor Buffer Set (BioLegend, Inc.). The tumor-infiltrating lymphocytes (TILs) were gated. Fluorescence data were acquired on a Beckman CytoFLEX and analyzed using Kaluza software 2.1.

**Statistical analysis.** The standard two-sample unpaired t-test was used to compare outcome differences in two-group experiments. One-way ANOVA followed by Tukey's multiple comparison test was applied to assess the statistical significance of differences among multiple treatment groups. The survival analysis of tumor-bearing mice was performed with Kaplan-Meier survival analysis. The log-rank (Mantel-Cox) test was used to obtain the P-values. Data are representative of three experiments and are presented as the mean. Error bars represent standard error of the mean. P<0.05 was considered to indicate a statistically significant difference.

## Results

*Lymphocytes mediating the immune response serve a pro-tumor role in MUC1-positive colon cancer.* High expression levels of MUC1 in tumor tissues are associated with poor prognosis in patients with breast cancer (5,9). However, to the best of our knowledge, it is unclear whether this association exists in colon cancer. The relationship between colon cancer survival time and MUC1 expression was analyzed. In the TCGA discovery dataset, the copy number of *MUC1* was used to determine the cut-off value of expression in tumor tissues as 0.118 (mean value of copy number). Patients with high and low expression levels of *MUC1* were identified for further analysis as  $\leq 0.1188$  for the low-*MUC1* group or  $> 0.118$  for the high-*MUC1* group. Kaplan-Meier survival analysis was performed to compare overall survival according to *MUC1* expression. The data suggested that the survival time in the low-*MUC1* group was improved compared with the high-*MUC1* group (Fig. 1A). To determine whether MUC1 promotes tumor cell proliferation, mouse CT26 and human SW480 colon cancer cell lines expressing human MUC1 were prepared. The MUC1<sup>+</sup> tumor cells were sorted by

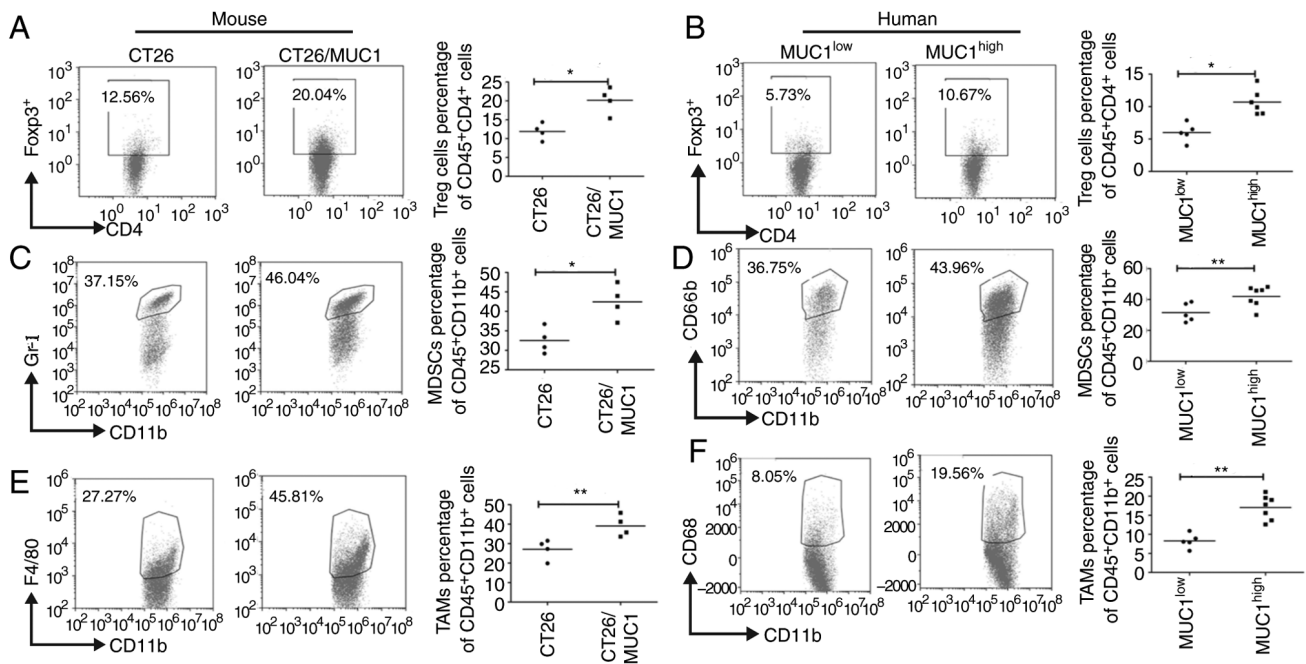


Figure 3. Immune-suppressive cells accumulate in MUC1-positive mouse (n=8) and human (n=12) tumor tissues. A single-cell suspension from tumor tissues was prepared and surface staining of immune cells was performed with flow cytometry. The percentages of (A) mouse and (B) human Treg cells (CD45<sup>+</sup>CD4<sup>+</sup>Foxp3<sup>+</sup>), (C) mouse MDSCs (CD45<sup>+</sup>CD11b<sup>+</sup>Gr-1<sup>+</sup>) and (D) human MDSCs (CD45<sup>+</sup>CD11b<sup>+</sup>CD66b<sup>+</sup>), and (E) mouse TAMs (CD45<sup>+</sup>CD11b<sup>+</sup>F4/80<sup>+</sup>) and (F) human TAMs (CD45<sup>+</sup>CD11b<sup>+</sup>CD68<sup>+</sup>) among tumor-infiltrating lymphocytes from mice and humans were assessed using flow cytometry. Data are representative of four experiments. Error bars represent the standard error of the mean. \*\*P<0.01 and \*P<0.05 vs. model control. MUC1, mucin1; MDSC, myeloid-derived suppressor cells; TAMs, tumor-associated macrophages; GR-1, Ly-6G/Ly-6C; F4/80 (EMR1), mucin-like receptor 1; Foxp3, forkhead box P3.

flow cytometry, and MUC1 expression in tumor cells was confirmed (Fig. 1B). Cell counting assays suggested that MUC1 itself did not significantly promote cell proliferation over 7 days (Fig. 1C and D). In a colon cancer animal model, MUC1-positive CT26 cells grew faster than MUC1-negative CT26 cells in murine models with intact immune competence (Figs. 1E; S1A and B). Additionally, it was found that the survival time in the MUC1-negative tumor-bearing BALB/c mice was improved compared with the MUC1-positive group (Fig. 1F). MUC1 expression on tumor cells that were isolated from the tumor-bearing mice was confirmed again by flow cytometry (Fig. S1C). However, there was no significant difference between the growth of MUC1-positive and MUC1-negative CT26 tumor cells in nu/nu mice (Fig. 1G). Furthermore, there was no significant difference between the growth of MUC1-positive and MUC1-negative SW480 tumor cells in murine models with lymphocyte deficiency (Figs. 1H; S1D and E). Additionally, there was no significant difference in the survival time between MUC1-positive and MUC1-negative tumor-bearing mice with lymphocyte deficiency (Fig. 1I). MUC1 expression on SW480 tumor cells that were isolated from the tumor-bearing mice was also confirmed by flow cytometry (Fig. S1F). This indicated that MUC1 might elicit a pro-tumor immune response. Additionally, no signs of weight loss were observed in any of the treatment groups (Fig. S1G-I).

*Increased accumulation of inflammatory cytokines in MUC1-positive tumor tissues.* Inflammation is known to be associated with the development of colon cancer (20,21). ELISA results measuring inflammatory cytokines in tumor-bearing mice suggested that IL-17A and IFN- $\gamma$  levels,

but not IL-10, TGF- $\beta$  and TNF- $\alpha$  levels, were significantly increased in MUC1-positive tissues compared with in MUC1-negative tissues (Fig. 2A). Subsequently, the expression levels of MUC1 in tumor tissue samples were assessed using IHC (Table I; Fig. 2B). High levels of IL-17A and IFN- $\gamma$  were observed in MUC1<sup>high</sup> tumor tissues, while the levels of IL-10, TGF- $\beta$  and TNF- $\alpha$  in MUC1<sup>high</sup> tumor tissues were not increased compared with those in MUC1<sup>low</sup> tumor tissues (Fig. 2C). To determine whether MUC1 augments or inhibits anti-MUC1 T-cell responses, tumor tissues from different groups of tumor-bearing mice or patients were harvested, weighed and analyzed by flow cytometry. CD45<sup>+</sup>CD3<sup>+</sup>CD4<sup>+</sup> T-cells, CD45<sup>+</sup>CD3<sup>+</sup>CD8<sup>+</sup> T-cells, CD45<sup>+</sup>CD11b<sup>+</sup>F4/80<sup>+</sup> cells and CD45<sup>+</sup>CD11b<sup>+</sup>GR1<sup>+</sup> cells were gated (Fig. S2). Intracellular cytokine staining analysis demonstrated that MUC1-positive and MUC1<sup>high</sup> tumor cells induced the production of intracellular IL-17A in CD4<sup>+</sup> T-cells (Fig. 2D and E) and IFN- $\gamma$  in CD8<sup>+</sup> T-cells (Fig. 2F and G). Since the killing of tumor cells by CD8<sup>+</sup> T cells is the principal mechanism of immune protection against tumors (22), the present study detected the number of granzyme B-producing CD8<sup>+</sup> T cells in tumor tissues. Notably, there was no significant increase in granzyme B-producing CD8<sup>+</sup> T cells in MUC1-positive and MUC1<sup>high</sup> tumor tissues (Fig. 2H and I). These results suggested that MUC1, as a tumor-associated antigen, does not enhance the cytotoxicity of cytotoxic T cells (CTLs), although it promotes an inflammatory response in the tumor microenvironment.

*Increased accumulation of immune-suppressive cells in MUC1-positive tumor tissues.* Tumor-infiltrating regulatory

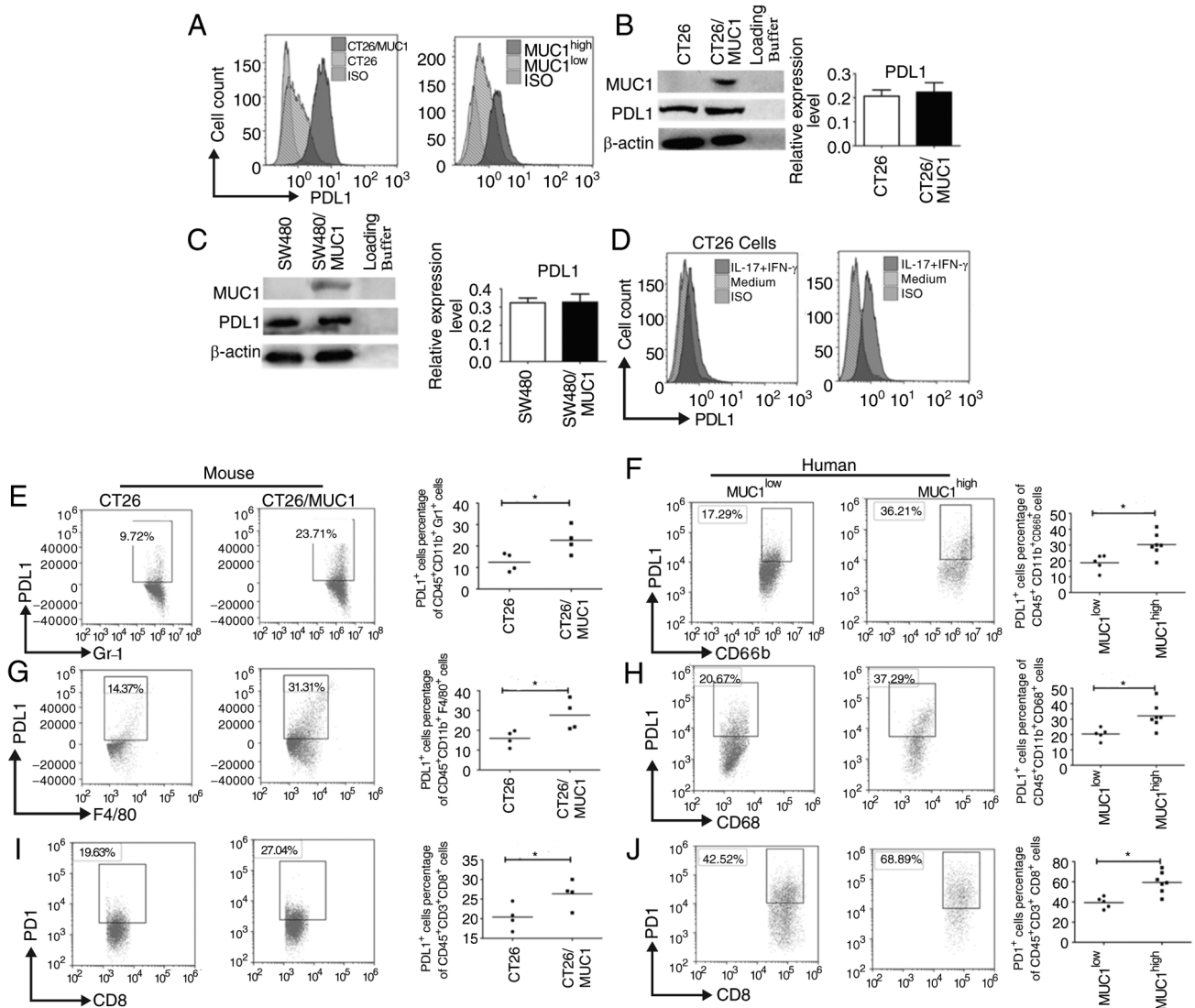


Figure 4. PDL1 expression on MDSCs, TAMs and tumor cells is greater in MUC1<sup>high</sup> tumor tissues from mice and patients. (A) Tumor cells from tumor-bearing mice or patients with colon cancer were isolated and PDL1 expression on the surface of tumor cells was assessed using flow cytometry. (B) CT26 and (C) SW480 tumor cells were transfected with *pcDNA3.1(-)/Myc-His-MUC1*. Semi-quantitative analysis of western blots of PDL1 expression in tumor cells after the transfection of *pcDNA3.1(-)/Myc-His-MUC1* using an anti-PDL1 mAb was performed.  $\beta$ -actin was used as an internal control. (D) CT26/vector and CT26/MUC1 cells were stimulated with mouse IFN- $\gamma$  (20 ng/ml) and IL-17A (10 ng/ml) for 48 h and surface PDL1 expression was assessed. PDL1 expression on the surface of (E) mouse and (F) human MDSCs and (G) mouse and (H) human TAMs in tumor tissues. PDL1 expression on the surface of (I) mouse and (J) human CD8<sup>+</sup>T cells in tumor tissues from tumor-bearing mice (n=8) or patients with colon cancer (n=12). Data are representative of four experiments. Error bars represent the standard error of the mean. \* $P < 0.05$  vs. model control. GR-1, Ly-6G/Ly-6C; F4/80 (EMR1), mucin-like receptor 1; PDL1, programmed death ligand 1; MDSC, myeloid-derived suppressor cells; TAM, tumor-associated macrophages; mAb, monoclonal antibody; MUC1, mucin1; ISO, isotype control.

T cells (Treg cells) are a major immune cell population that contribute to the establishment of an immunosuppressive tumor microenvironment, to hamper the development of effective antitumor immunity, and are often associated with poor prognosis (23). Significantly more CD4<sup>+</sup> Foxp3<sup>+</sup> Tregs were observed to infiltrate MUC1-positive and MUC1<sup>high</sup> tumor tissues compared with MUC1-negative and MUC1<sup>low</sup> tumor tissues ( $P < 0.05$ ; Fig. 3A and B). Furthermore, tumor growth is associated with the accumulation of MDSCs and TAMs, where these cells facilitate tumor immune escape by inhibiting anti-tumor immune responses (22). The present results indicated that significantly more MDSCs (Fig. 3C and D) and TAMs (Fig. 3E and F) accumulated in MUC1-positive and MUC1<sup>high</sup> tumor tissues ( $P < 0.05$ ).

*PDL1 expression on MDSCs, TAMs and tumor cells is greater in MUC1<sup>high</sup> tumor tissues from mice and patients.* PDL1 has previously been demonstrated to exhaust CTLs by binding PDI (24,25). PDL1 expression was upregulated on tumor cells from MUC1-positive and MUC1<sup>high</sup> tumor tissues (Fig. 4A). However, in CT26 and SW480 cells transfected with the MUC1-expressing plasmid, MUC1 did not appear to promote PDL1 expression on tumor cells (Fig. 4B and C). These data indicated that PDL1 expression in MUC1-positive and MUC1<sup>high</sup> tumor tissues was upregulated due to other mechanisms. Since the present data also indicated that inflammatory cytokines were elevated in MUC1<sup>high</sup> tumor tissues, it is unclear whether high PDL1 expression on tumor cells was caused by these inflammatory cytokines. IL-17A and



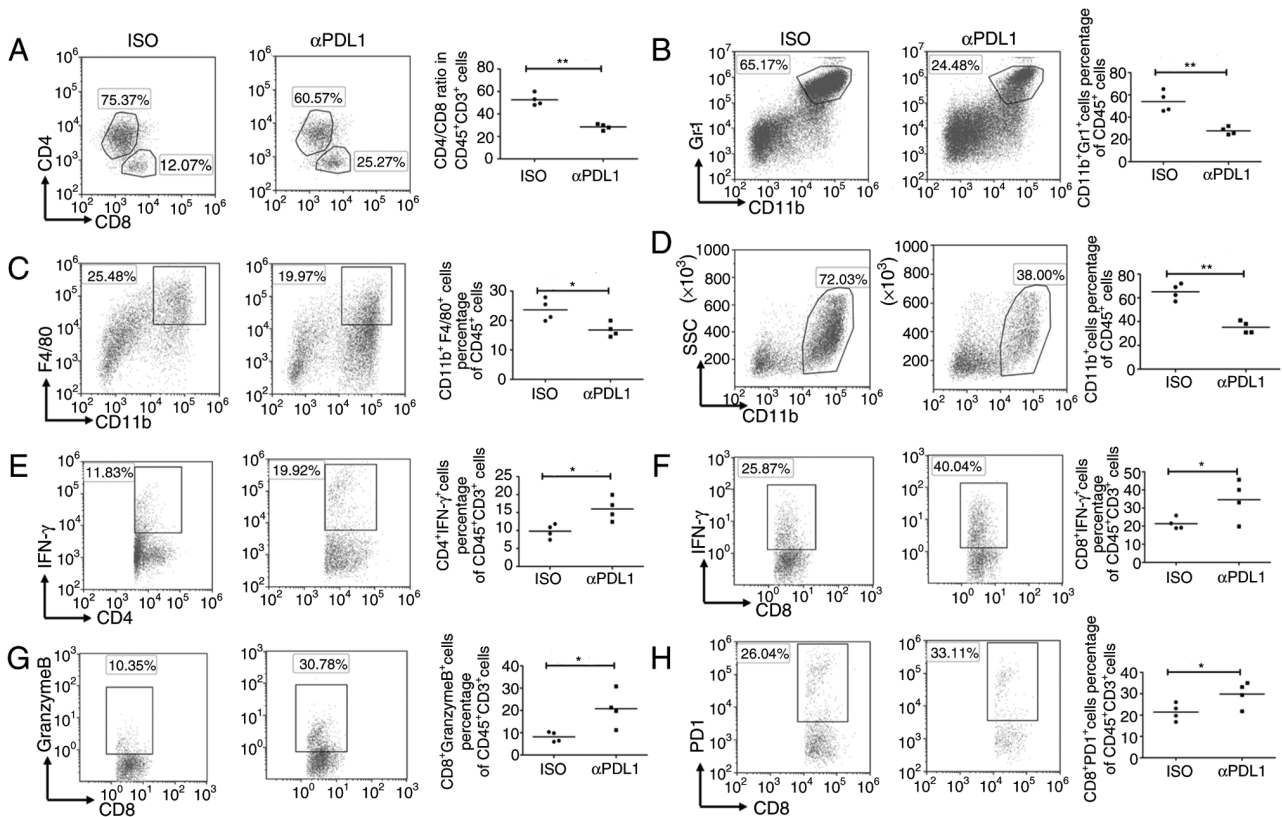


Figure 5. Targeting PDL1 influences the immunogenic tumor microenvironment. Mice were subcutaneously challenged with  $1 \times 10^6$  CT26/MUC1 tumor cells. After 7 days, the mice were injected intraperitoneally with an anti-PDL1 antibody (200  $\mu\text{g}/\text{mouse}$ ;  $n=4$ ), or control-IgG (200  $\mu\text{g}/\text{mouse}$ ;  $n=4$ ). Antibody treatments were administered an additional three times every 3 days after CT26/MUC1 inoculation. Surface staining patterns of (A) T-cells (CD45<sup>+</sup>CD4<sup>+</sup>, CD45<sup>+</sup>CD8<sup>+</sup>), (B) myeloid-derived suppressor cells (CD45<sup>+</sup>CD11b<sup>+</sup>Gr1<sup>+</sup>), (C) tumor-associated macrophages (CD45<sup>+</sup>CD11b<sup>+</sup>F4/80<sup>+</sup>) and (D) myeloid-derived cells (CD45<sup>+</sup>CD11b<sup>+</sup>) in tumor tissues were analyzed using flow cytometry. TILs in tumor tissues from tumor-bearing mice were stimulated with phorbol-12-myristate-13-acetate and ionomycin in the presence of brefeldin A for 4 h. (E) Percentages of IFN- $\gamma$ <sup>+</sup> T-cells among CD4<sup>+</sup>CD45<sup>+</sup> TILs. (F) Percentages of IFN- $\gamma$ <sup>+</sup> T-cells among CD8<sup>+</sup>CD45<sup>+</sup> TILs. (G) Percentages of granzyme B<sup>+</sup> T-cells among CD8<sup>+</sup>CD45<sup>+</sup> TILs. (H) PD1 expression on the surface of CD8<sup>+</sup> T-cells in tumor tissues from tumor-bearing mice. Data are representative of four experiments. Error bars represent the standard error of the mean. \*\* $P < 0.01$  and \* $P < 0.05$  vs. model control. GR-1, Ly-6G/Ly-6C; F4/80 (EMR1), mucin-like receptor 1; TIL, tumor-infiltrating lymphocytes; PDL1, programmed death ligand 1; PD1, programmed cell death 1; ISO, isotype control; MUC1, mucin1.

IFN- $\gamma$  stimulation promoted PDL1 expression on CT26 cells, as well as CT26/MUC1 cells (Fig. 4D), which suggests that increased inflammatory cytokine levels could promote PDL1 expression on CT26/MUC1 cells. Since PDL1 is expressed on tumor cells and antigen-presenting cells, the present study assessed whether PDL1 expression was increased on MDSCs and TAMs. PDL1 expression on MDSCs and TAMs was significantly elevated in MUC1<sup>high</sup> tumor tissues from mice and humans (Fig. 4E-H). Since PD1 expression on T-cells is similarly critical for activation of the PDL1-PD1 signaling pathway (25), PD1 expression on CD8<sup>+</sup> T-cells was also measured. PD1 staining was analyzed by FACS, and the results revealed that PDL1 expression, in both mouse and human CD8<sup>+</sup> T-cells, was significantly increased (Fig. 4I and J). This suggested that more inhibitory immune cells and checkpoint molecules accumulated in MUC1<sup>high</sup> tumor tissues from mice and patients.

**Targeting PDL1 induces an antitumor immune response.** Flow cytometry analysis of TILs in anti-PDL1 antibody-treated tumors indicated that the ratio of CD4/CD8 T cells was significantly decreased after antibody treatment compared with that in isotype antibody-treated tumors (Fig. 5A). Furthermore,

the present study revealed that the proportions of MDSCs and TAMs were significantly lower in mice treated with anti-PDL1 antibodies than in control-treated mice (Fig. 5B and C). Notably, the percentage of myeloid-derived cells (CD11b<sup>+</sup> cells) was also significantly lower in mice treated with anti-PDL1 antibodies compared with the control-treated mice (Fig. 5D). Using the PDL1 antibody to target PDL1 led to significantly greater proportions of IFN- $\gamma$ -producing CD8<sup>+</sup> T cells, granzyme B-producing CD8<sup>+</sup> T cells and IFN- $\gamma$ -producing CD4<sup>+</sup> T cells compared with those in the controls (Fig. 5E-G). The percentage of PD1<sup>+</sup> CD8<sup>+</sup> T cells was also significantly greater in mice injected with the PDL1 antibody (Fig. 5H). These results indicated that targeting PDL1 reduces the percentage of inhibitory immune cells and enhances the activity and cytotoxicity of T cells in MUC1-positive colon cancer models; therefore, targeting PDL1 in MUC1-positive tumor has the potential to change the tumor immunosuppressive microenvironment.

**Targeting PDL1 induces antitumor effects.** Since PDL1-targeting in MUC1-positive tumor tissues was revealed to enhance the T-cell response, the present study next aimed to determine whether antibody treatment with anti-PDL1



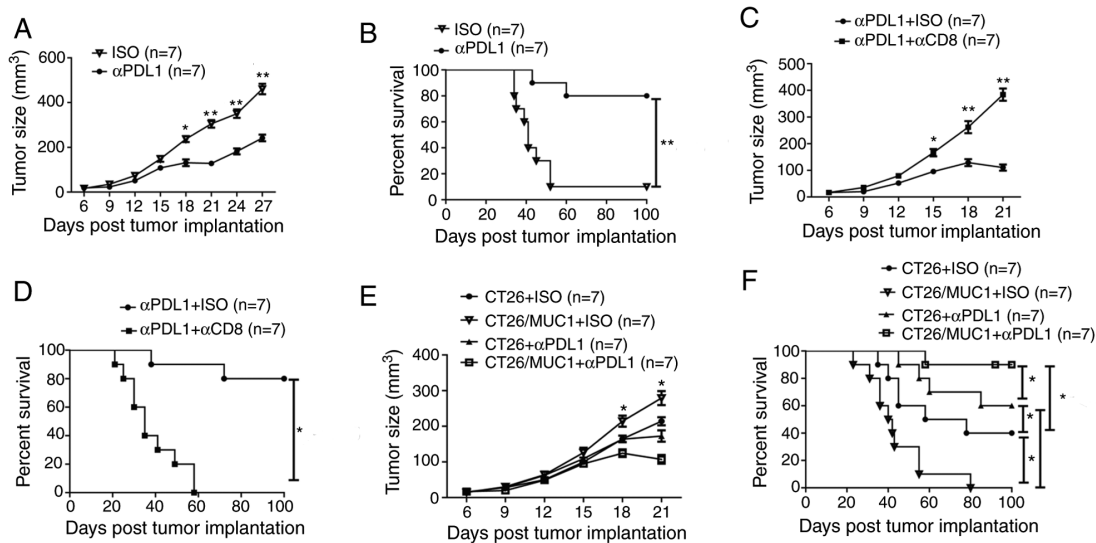


Figure 6. Targeting PDL1 induces significant antitumor effects. After mouse tumor diameters reached 3–4 mm, the mice were injected four times at 3-day intervals with isotype control mouse antibodies or an anti-PDL1 antibody. (A) Tumor growth and (B) survival rates were recorded (n=7). After mouse tumor diameters reached 3–4 mm, mice were injected intraperitoneally with anti-CD8 (500  $\mu$ g) or isotype control mouse antibodies (250  $\mu$ g) on day 3. Mice were then injected with an anti-PDL1 antibody. The anti-CD8 or isotype control mouse antibodies were further injected 3 days before anti-PDL1 injection. (C) Tumor growth and (D) survival were recorded (n=7). The (E) tumor growth and (F) survival rates of mice injected with  $1 \times 10^6$  CT26/vector or CT26/MUC1 tumor cells were recorded (n=7). Error bars represent the standard error of the mean. \*\*P<0.01 and \*P<0.05 vs. model control. MUC1, mucin1; PDL1, programmed death ligand 1; ISO, isotype control.

could strengthen antitumor immunity. The data suggested that anti-PDL1 antibody treatment could significantly inhibit the growth of tumors on day 18, 21, 24 and 27 after tumor implantation, and prolong the survival time of tumor-bearing mice compared with the control antibody (Figs. 6A and B; S3A and B). To explore the cellular mechanisms underlying antitumor immunity, CD8<sup>+</sup> T cells in the mice were depleted during PDL1 antibody treatment. Mice with depleted CD8<sup>+</sup> cells lost the protective antitumor effects induced by the PDL1 antibody (Fig. 6C and D). These findings suggest that CD8<sup>+</sup> T cells are critical for the antitumor immune responses elicited by PDL1 antibodies. Additionally, no signs of weight loss were observed in any of the treatment groups (Fig. S3C; data not shown for anti-PDL1+anti-CD8). As more CD8<sup>+</sup> and CD4<sup>+</sup> T cells were attracted to the tumor site in MUC1-positive tumor-bearing mice (Fig. 2C–G), despite the antitumor immune response of these immune cells being diminished by the PDL1-PDL1 signaling pathway, the present study also determined whether stronger antitumor immunity in MUC1-positive tumor-bearing mice could be elicited by anti-PDL1 antibody treatment, as compared with that in MUC1-negative tumor-bearing mice. Notably, MUC1-positive tumor-bearing mice had larger tumors and shorter survival times than MUC1-negative tumor-bearing mice, but MUC1-positive tumor-bearing mice injected with anti-PDL1 antibodies had smaller tumors and significantly longer survival times than MUC1-negative tumor-bearing mice injected with anti-PDL1 antibodies (Fig. 6E and F). These data suggest that targeting of PDL1 using PDL1 antibodies in MUC1-positive tumor-bearing mice is necessary to effectively elicit an antitumor immune response.

## Discussion

The heterodimeric MUC1 protein is aberrantly upregulated in colon cancer and has been used as a candidate target antigen

in peptide, dendritic cell and whole tumor vaccines (6). High expression levels of MUC1 have been linked to poor outcomes in colon cancer (5,7). However, the relationship between MUC1 upregulation and antitumor immune response in the tumor microenvironment is unclear. The present study demonstrated that MUC1 has a pro-tumor role in immune-competent mice, and that Tregs, MDSCs and TAMs accumulate in MUC1-positive tumor tissues. Furthermore, MUC1-positive tumor cells were found to promote PDL1 expression on tumor cells, MDSCs and TAMs by attracting more inflammatory cytokines and suppressing the antitumor immune response. Finally, targeting PDL1 in MUC1-positive tumor-bearing mice was demonstrated to transform the tumor microenvironment, enhance the antitumor immune response and inhibit tumor growth.

Tumor-infiltrating myeloid cells and pro-inflammatory cytokines promote the development of colorectal carcinoma (26). Tumor-associated inflammation, manifested based on IL-17 expression, is of great importance for the pathogenesis of colorectal carcinoma (27,28). The present study observed greater IL-17A production in MUC1-positive tumor tissues than in MUC1-negative tumor tissues. Since tumor tissues tend to attract inflammatory cytokines during an immune response (29), it is feasible that high expression levels of IL-17A in MUC1-positive tumor tissues might be specific to the tumor-associated antigen MUC1, but the mechanisms responsible for this effect have not been addressed. Notably, the present data also suggested that the expression levels of IFN- $\gamma$  and the percentage of IFN- $\gamma$ -producing CD8<sup>+</sup> T cells were also greater in MUC1-positive tumor tissues compared with in MUC1-negative tumor tissues, although the percentage of granzyme B-producing CD8<sup>+</sup> T cells was unchanged. IFN- $\gamma$  and IFN- $\gamma$ -producing CD8<sup>+</sup> T cells serve a pivotal role in the killing of tumor cells, but a high level of IFN- $\gamma$  can also impair the cytotoxicity of CD8<sup>+</sup> T cells and

result in T-cell exhaustion (30). Immunosuppressive cells promote tumor immune escape by inducing immunosuppression and accumulate in tumors where they exert T-cell immunosuppression (31,32). When analyzing Treg cells, MDSCs and TAMs in tumor tissues, more inhibitory immune cells were found to accumulate in MUC1-positive tumor tissues than in MUC1-negative tumor tissues, and thus, it was hypothesized that this might represent a mechanism by which MUC1-positive and MUC1<sup>high</sup> tumor cells escape immune surveillance.

MUC1 is a ligand for sialoadhesin, which is a macrophage-restricted adhesion molecule, and as such, might be involved in the recruitment of macrophages to the tumor site (4). This could be why macrophages are attracted to tumor sites in colon cancer (5,9). It is also possible that the large numbers of inhibitory immune cells neutralized the antitumor immune response of IFN- $\gamma$ -producing CD8<sup>+</sup> T-cells.

High PDL1 expression on tumor cells or myeloid cells is associated with poor prognosis compared with PDL1-negative tumors (33,34). MUC1 can promote PDL1 expression via the recruitment of MYC and NF- $\kappa$ B p65 to the *PDL1* promoter in certain solid tumors, such as triple-negative breast cancer, where they contribute to an aggressive pathogenesis (35). Additionally, PDL1 expression is associated with high expression levels of inflammatory factors, such as IFN- $\gamma$  and IL-17A, because these cytokines can stimulate tumor cells or myeloid cells to produce PDL1 and then suppress the cytotoxicity of tumor-specific T cells (15,36). The present data indicates that MUC1 did not directly promote PDL1 expression on colon cancer cells, but IL-17A, IFN- $\gamma$  and myeloid cells were more attracted to MUC1-positive tumor tissues than MUC1-negative tumor tissues, which emphasizes the importance of exploring the mechanism through which these inhibitory immune cells and inflammatory cytokines promote the growth of MUC1-positive tumor cells. IL-17A and IFN- $\gamma$  were observed to enhance PDL1 expression on CT26/MUC1 and SW480/MUC1 tumor cells more so than MUC1 itself, and high PDL1 expression was observed on MDSCs and TAMs. This might be because MUC1-positive tumor cells recruit robust inflammatory cytokines and enhance PDL1 expression on tumor cells and myeloid cells. Overall, MUC1 promoted PDL1 expression on tumor cells through the recruitment of inflammatory cytokines and then inhibited the antitumor immune response via the PDL1/PD1 signaling pathway, enabling the evasion of immune surveillance.

Targeting PDL1 on tumor cells, MDSCs and macrophages can suppress the growth of tumor cells (37-40). While it is possible to restore the tumor microenvironment and suppress tumor cell growth by blocking the PDL1-PD1 signaling pathway, it was found that this approach in MUC1-positive tumor-bearing mice promoted the infiltration of IFN- $\gamma$ -producing CD8<sup>+</sup> T-cells and inhibited the infiltration of myeloid cells, MDSCs and TAMs in the tumor microenvironment. This is pivotal to transform the tumor immunosuppressive microenvironment and enhance anti-tumor immune responses in favor of tumor eradication (41), since the presence of a high number of CD8<sup>+</sup> T lymphocytes and fewer MDSCs and TAMs in tumor tissues is associated with improved prognosis (42,43). Interestingly, the present

findings also suggest that targeting PDL1 in MUC1-positive tumor-bearing mice inhibited tumor growth and elicited a stronger antitumor effect than that in MUC1-negative tumor-bearing mice. This provides further *in vivo* evidence of the tumor suppressor function of PDL1 (44-46).

Notably, the present study only investigated the status of immune cells in MUC1-positive and MUC1-negative tumor tissues, and further studies are required to explore the mechanism through which MUC1 upregulation promotes the accumulation of suppressive immune cells in MUC1-positive tumor tissues. In summary, the present study demonstrated a pro-tumor role of MUC1 with important implications for MUC1-positive colorectal cancer, and provides a foundation for the application of PDL1 inhibitors to MUC1-positive colon cancer.

### Acknowledgements

Not applicable.

### Funding

The present work was supported by grants from the Leader Training Program in Medical Subjects of Health and Family Planning Commission of Yunnan Province (grant no. D-201657) and the Scientific Research Fund General Projects of Yunnan Provincial Department of Education (grant no. 2015Y150).

### Availability of data and materials

All data generated or analyzed during this study are included in this published article.

### Authors' contributions

YHZ and XD performed the immunoassays and drafted the manuscript. LB and XS collected the patient samples and performed the statistical analysis. YJZ designed the study and helped to revise the manuscript. All authors read and approved the final manuscript.

### Ethics approval and consent to participate

The treatment of mice was approved by the Institutional Animal Care and Use Committee of Kunming Medical University (approval no. KMU20170121). The patient research was approved by the Ethics Committee of The First Affiliated Hospital of Kunming Medical University (approval no. KMU20160901) and conformed with the ethical standards of the World Medical Association Declaration of Helsinki. All patients provided written informed consent.

### Patient consent for publication

Not applicable.

### Competing interests

The authors declare that they have no competing interests.

## References

- Chen W, Zheng R, Baade PD, Zhang S, Zeng H, Bray F, Jemal A, Yu XQ and He J: Cancer statistics in China, 2015. *CA Cancer J Clin* 66: 115-132, 2016.
- Ahmad R, Alam M, Hasegawa M, Uchida Y, Al-Obaid O, Kharbada S and Kufe D: Targeting MUC1-C inhibits the AKT-S6K1-eIF4A pathway regulating TIGAR translation in colorectal cancer. *Mol Cancer* 16: 33, 2017.
- Kasprzak A, Siodła E, Andrzejewska M, Szejma J, Seraszek-Jaros A, Cofta S and Szaflarski W: Differential expression of mucin 1 and mucin 2 in colorectal cancer. *World J Gastroenterol* 24: 4164-4177, 2018.
- Singh R and Bandyopadhyay D: MUC1: A target molecule for cancer therapy. *Cancer Biol Ther* 6: 481-486, 2007.
- Taylor-Papadimitriou J, Burchell J, Miles DW and Dalziel M: MUC1 and cancer. *Biochim Biophys Acta* 1455: 301-313, 1999.
- Nath S and Mukherjee P: MUC1: A multifaceted oncoprotein with a key role in cancer progression. *Trends Mol Med* 20: 332-342, 2014.
- Guo M, You C and Dou J: Role of transmembrane glycoprotein mucin 1 (MUC1) in various types of colorectal cancer and therapies: Current research status and updates. *Biomed Pharmacother* 107: 1318-1325, 2018.
- Smith JS, Colon J, Madero-Visbal R, Isley B, Konduri SD and Baker CH: Blockade of MUC1 expression by glycerol guaiacolate inhibits proliferation of human breast cancer cells. *Anticancer Agents Med Chem* 10: 644-6650, 2010.
- Apostolopoulos V, Pietersz GA and McKenzie IF: MUC1 and breast cancer. *Curr Opin Mol Ther* 1: 98-103, 1999.
- Yang E, Hu XF and Xing PX: Advances of MUC1 as a target for breast cancer immunotherapy. *Histol Histopathol* 22: 905-922, 2007.
- Agrawal B, Krantz MJ, Reddish MA and Longenecker BM: Cancer-associated MUC1 mucin inhibits human T-cell proliferation, which is reversible by IL-2. *Nat Med* 4: 43-49, 1998.
- van de Wiel-van Kemenade E, Ligtenberg MJ, de Boer AJ, Buijs F, Vos HL, Melief CJ, Hilkens J and Figdor CG: Episialin (MUC1) inhibits cytotoxic lymphocyte-target cell interaction. *J Immunol* 151: 767-776, 1993.
- Topalian SL, Drake CG and Pardoll DM: Targeting the PD-1/B7-H1(PD-L1) pathway to activate anti-tumor immunity. *Curr Opin Immunol* 24: 207-212, 2012.
- Tang J, Yu JX, Hubbard-Lucey VM, Neftelinov ST, Hodge JP and Lin Y: Trial watch: The clinical trial landscape for PDI/PDL1 immune checkpoint inhibitors. *Nat Rev Drug Discov* 17: 854-855, 2018.
- Ma YF, Chen C, Li D, Liu M, Lv ZW, Ji Y and Xu J: Targeting of interleukin (IL)-17A inhibits PDL1 expression in tumor cells and induces anticancer immunity in an estrogen receptor-negative murine model of breast cancer. *Oncotarget* 5: 7614-7624, 2017.
- Baldus SE, Engelmann K and Hanisch FG: MUC1 and the MUCs: A family of human mucins with impact in cancer biology. *Crit Rev Clin Lab Sci* 41: 189-231, 2004.
- Goldman MJ, Craft B, Hastie M, Repečka K, McDade F, Kamath A, Banerjee A, Luo Y, Rogers D, Brooks AN, *et al*: Visualizing and interpreting cancer genomics data via the Xena platform. *Nat Biotechnol* 38: 675-678, 2020.
- Cancer Genome Atlas Network: Comprehensive molecular characterization of human colon and rectal cancer. *Nature* 487: 330-337, 2012.
- Helfinger V, Henke N, Harenkamp S, Walter M, Epah J, Penski C, Mittelbronn M and Schröder K: The NADPH oxidase Nox4 mediates tumour angiogenesis. *Acta Physiol (Oxf)* 216: 435-446, 2016.
- Koboziev I, Karlsson F and Grisham MB: Gut-associated lymphoid tissue, T cell trafficking, and chronic intestinal inflammation. *Ann N Y Acad Sci* 1207 (Suppl 1): E86-E93, 2010.
- Terzić J, Grivnenikov S, Karin E and Karin M: Inflammation and colon cancer. *Gastroenterology* 138: 2101-2114.e5, 2010.
- Gajewski TF, Schreiber H and Fu YX: Innate and adaptive immune cells in the tumor microenvironment. *Nat Immunol* 14: 1014-1022, 2013.
- Villarreal DO, L'Huillier A, Armington S, Mottershead C, Filippova EV, Coder BD, Petit RG and Princiotta MF: Targeting CCR8 induces protective antitumor immunity and enhances vaccine-induced responses in colon cancer. *Cancer Res* 78: 5340-5348, 2018.
- Amarnath S, Mangus CW, Wang JC, Wei F, He A, Kapoor V, Foley JE, Massey PR, Felizardo TC, Riley JL, *et al*: The PDL1-PD1 axis converts human TH1 cells into regulatory T cells. *Sci Transl Med* 3: 111ra120, 2011.
- Dong H, Strome SE, Salomao DR, Tamura H, Hirano F, Flies DB, Roche PC, Lu J, Zhu G, Tamada K, *et al*: Tumor-associated B7-H1 promotes T-cell apoptosis: A potential mechanism of immune evasion. *Nat Med* 8: 793-800, 2002.
- Beatty P, Ranganathan S and Finn OJ: Prevention of colitis-associated colon cancer using a vaccine to target abnormal expression of the MUC1 tumor antigen. *Oncoimmunology* 1: 263-270, 2012.
- Dmitrieva-Posocco O, Dzutsev A, Posocco DF, Hou V, Yuan W, Thovarai V, Mufazalov IA, Gunzer M, Shilovskiy IP, Khaitov MR, *et al*: Cell-type-specific responses to interleukin-1 control microbial invasion and tumor-elicited inflammation in colorectal cancer. *Immunity* 50: 166-180.e7, 2019.
- Wang K and Karin M: Tumor-elicited inflammation and colorectal cancer. *Adv Cancer Res* 128: 173-196, 2015.
- Chen J, Pitmon E and Wang K: Microbiome, inflammation and colorectal cancer. *Semin Immunol* 32: 43-53, 2017.
- Farhood B, Najafi M and Mortezaee K: CD8<sup>+</sup> cytotoxic T lymphocytes in cancer immunotherapy: A review. *J Cell Physiol* 234: 8509-8521, 2019.
- Bianchi G, Borgonovo G, Pistoia V and Raffaghello L: Immunosuppressive cells and tumour microenvironment: Focus on mesenchymal stem cells and myeloid derived suppressor cells. *Histol Histopathol* 26: 941-951, 2011.
- Liu Y and Cao X: Immunosuppressive cells in tumor immune escape and metastasis. *J Mol Med (Berl)* 94: 509-522, 2016.
- Muenst S, Schaerli AR, Gao F, Däster S, Trella E, Droeser RA, Muraro MG, Zajac P, Zanetti R, Gillanders WE, *et al*: Expression of programmed death ligand 1 (PD-L1) is associated with poor prognosis in human breast cancer. *Breast Cancer Res Treat* 146: 15-24, 2014.
- Sabatier R, Finetti P, Mamessier E, Adelaide J, Chaffanet M, Ali HR, Viens P, Caldas C, Birnbaum D and Bertucci F: Prognostic and predictive value of PDL1 expression in breast cancer. *Oncotarget* 6: 5449-5464, 2015.
- Maeda T, Hiraki M, Jin C, Rajabi H, Tagde A, Alam M, Bouillez A, Hu X, Suzuki Y, Miyo M, *et al*: MUC1-C induces PD-L1 and immune evasion in triple-negative breast cancer. *Cancer Res* 78: 205-215, 2018.
- Pardoll DM: The blockade of immune checkpoints in cancer immunotherapy. *Nat Rev Cancer* 12: 252-264, 2012.
- Curiel TJ, Wei S, Dong H, Alvarez X, Cheng P, Mottram P, Krzysiek R, Knutson KL, Daniel B, Zimmermann MC, *et al*: Blockade of B7-H1 improves myeloid dendritic cell-mediated antitumor immunity. *Nat Med* 9: 562-567, 2003.
- Ghebeh H, Tulbah A, Mohammed S, Elkum N, Bin Amer SM, Al-Tweigeri T and Dermime S: Expression of B7-H1 in breast cancer patients is strongly associated with high proliferative Ki-67-expressing tumor cells. *Int J Cancer* 121: 751-758, 2007.
- Liu Y, Zeng B, Zhang Z, Zhang Y and Yang R: B7-H1 on myeloid-derived suppressor cells in immune suppression by a mouse model of ovarian cancer. *Clin Immunol* 129: 471-481, 2008.
- Parsa AT, Waldron JS, Panner A, Crane CA, Parney IF, Barry JJ, Cachola KE, Murray JC, Tihan T, Jensen MC, *et al*: Loss of tumor suppressor PTEN function increases B7-H1 expression and immunoresistance in glioma. *Nat Med* 13: 84-88, 2007.
- Xiao W, Ibrahim ML, Redd PS, Klement JD, Lu C, Yang D, Savage NM and Liu K: Loss of Fas expression and function is coupled with colon cancer resistance to immune checkpoint inhibitor immunotherapy. *Mol Cancer Res* 17: 420-430, 2019.
- Noy R and Pollard JW: Tumor-associated macrophages: From mechanisms to therapy. *Immunity* 41: 49-61, 2014.
- Wherry EJ: T cell exhaustion. *Nat Immunol* 12: 492-499, 2011.
- Lucas J, Hsieh TC, Halicka HD, Darzynkiewicz Z and Wu JM: Upregulation of PD-L1 expression by resveratrol and piceatannol in breast and colorectal cancer cells occurs via HDAC3/p300-mediated NF- $\kappa$ B signaling. *Int J Oncol* 53: 1469-1480, 2018.
- Stenhjem DD, Tran D, Nkrumah MA and Gupta S: PDI/PDL1 inhibitors for the treatment of advanced urothelial bladder cancer. *Onco Targets Ther* 11: 5973-5989, 2018.
- Zheng A, Li F, Chen F, Zuo J, Wang L, Wang Y, Chen S, Xiao B and Tao Z: PD-L1 promotes head and neck squamous cell carcinoma cell growth through mTOR signaling. *Oncol Rep* 41: 2833-2843, 2019.

